NATIONAL ADVISORY COMMITTEE FOR AERONAUTICS

TECHNICAL MEMORANDUM

No. 1171

LABORATORY REPORT ON THE INVESTIGATION OF THE FLOW AROUND TWO TURBINE-BLADE PROFILES USING THE INTERFEROMETER METHOD

By K. von Vietinghoff-Scheel

Translation

"Versuchsbericht über die Untersuchung der Strömung um zwei Turbinenschaufelprofile mit Hilfe der Interferenzmethode." Deutsche Luftfahrtforschung, Untersuchungen und Mitteilungen Nr. 2096
Luftfahrtforschungsanstalt Hermann Göring E. V.
Institut für Motorenforschung, Braunschweig, Germany, ZWB
May 31, 1944

Washington
July 1947

NATIONAL ADVISORY COMMITTEE FOR AERONAUTICS

TECHNICAL MEMORANDUM NO. 1171

LABORATORY REPORT ON THE INVESTIGATION OF THE FLOW AROUND TWO TURBINE-BLADE PROFILES USING THE INTERFEROMETER METHOD*

By K. von Vietinghoff-Scheel

I. PURPOSE AND AIM OF INVESTIGATION

At the request of the Junkers Aircraft and Engine Construction Company, Engine Division, Dessau Main Plant, an investigation was made using the interferometer method on the two turbine-blade profiles submitted.

The interferometer method (reference 1) enables making visible the differences in density and consequently the boundary layers that develop when a flow is directed on the profile. Recognition of the points on the profile at which separation of flow occurs is thus possible. By means of the interference photographs the extent of the dead-water region may be ascertained. The size of the dead-water region provides evidence as to the quality of the flow and allows a qualitative estimate of the amount of the flow losses. Interference photographs thus provide means of judging the utility of profiles under specific operating conditions and provide suggestions for possible changes of profile contours that might help to improve flow relations. Conclusions may be drawn concerning the influence of the blade-spacing ratio, the inlet-air angle, and the connection between the curvature of the profile contour and the point of separation of the flow from the profile surface.

In addition, interference photographs also make possible ascertainment of the distribution of pressure and velocity over the blade. Such quantitative evaluation of the interference photographs was not undertaken in regard to the present experiments.

---

*"Versuchsbericht über die Untersuchung der Strömung um zwei Turbinenschaufelprofile mit Hilfe der Interferenzmethode," Deutsche Luftfahrtforschung, Untersuchungen und Mitteilungen Nr. 2096, Luftfahrtforschungsanstalt Hermann Göring E. V., Inst. f. Motorenforschung, Braunschweig, Germany, ZWB, May 31, 1944.

The rotor blade midspan sections for "I" and for "III" were investigated. Hereinafter the first blade will be designated profile I and the second, profile II.

From the data submitted, it appears that the blade sections operate in the turbine under the following conditions: t, cascade spacing; l, blade chord measured as the normal projection on a straight line tangent to the concave side of the blade; β_1, inlet-air angle [NACA comment: As specifically defined in next paragraph]; β_2, exit angle:

	t/l	β_1	β_2	Re
Profile I	0.676	30-33°	34.6°	~250,000
Profile II	.676	30-33°	35.5°	

II. SETUP AND CONDITIONS OF EXPERIMENTS

Figure 1 shows the Zehnder-Mach interferometer and the cascade tunnel in which the blades were installed for the investigations. In figure 2 are shown cross sections of the tunnel, which can be used for investigations involving inlet-air angles from $\beta_1 = 20°$ to $\beta_1 = 90°$ and turning angles β_u between 36° and 145°. "Inlet-air angle" is here defined as the angle between the cascade line and the direction of the incident air flow, at the cascade line; the direction pointing from the pressure side to the suction side of the profile is designated the positive direction.

The air is sucked by an exhauster through the inlet duct a, which is square in cross section and provided with an entrance fairing (figs. 2(a) and 2(b)). The air then flows through the two-dimensional cascade b. The air stream freely emerging from the cascade is collected by the collecting funnel c and led to the exhauster through the diffuser d and a duct elbow attached to the diffuser by a flexible leather sleeve. The front and rear walls f of the air channel ahead of the cascade can swing about the two axes g. Thus the cascade can be investigated in operation at various inlet-air angles. For each inlet-air angle a different inlet duct a may be attached to the cascade tunnel. Also, for each exit angle a different diffuser can be bolted to the base plate of the tunnel. During each experiment, the diffuser is shifted on the base plate until equal static pressure exists in both dead spaces m and n. The two windows i are built into the strong

side walls h of the cascade tunnel in parallel planes. (See fig. 2(b).) The blades b are held firmly in the tunnel by two tension wires k of 2-millimeter diameter and are kept from contact with the glass windows by rubber pads l glued to the ends. (See fig. 2(b).)

The model blades were manufactured here from commercially processed beech wood. In making the blades, special emphasis was laid on keeping the spanwise sections the same. The surface of the model blades was lacquered.

The spacing ratio $t/l = 0.676$ could not actually be attained with the model blades in the air channel. Therefore, profiles I and II were each investigated at two spacing ratios t/l, namely, profile I at $t/l = 0.658$ and 0.824 and profile II at $t/l = 0.638$ and 0.800. In order to obtain a better survey of the behavior of the two profiles, the range of inlet-air angles was extended in both directions.

In most of the experiments hereinafter described, one blade of the cascade was slightly heated. For this purpose the blade was provided with a hole o (figs. 2(a) and 2(b)) into which was inserted a heating coil wound on a ceramic tube. In the photographs, the shadow of the electric cord leading to this heater is visible. The position of this cord changes with the inlet-air angle. Its direction agrees very exactly with that of the incident flow ahead of the cascade. Theoretical considerations indicate that the flow field is not influenced by temperature differences if the characteristics of the fluid (density and viscosity) are independent of temperature. Because the temperature differences arising in this case between the blade surface and the air flowing past do not, on the basis of the investigations, amount to more than 20° C, the heating can have no marked effect on the boundary layer and its points of separation.

III. DISCUSSION OF INTERFERENCE PHOTOGRAPHS

Figure 3 shows an interference photograph with no air flow in the test tunnel. The interference bands run as straight lines parallel to one another. The black shadows seen in the two right-hand corners of most of the photographs are simply the frame of the observation window. When a flow occurs around the blades, a field of density variation arises. Thereby the bands are deflected from their original positions in proportion to the local density differences. In potential flow, a continuous curvature of the

bands occurs as a result of adiabatic change of state; these bands may be noted particularly near the stagnation point because of the more pronounced pressure and density changes occurring there. A bend occurs in the bands at the boundary layer because of the temperature rise produced by friction. Ascertainment of the development of the boundary layer along the profile surface and the point of separation is thus possible. In certain cases it is impossible to decide without further evidence whether what is observed is a thickened boundary layer or a partial separation of the flow. The dead-water region is usually characterized by bands running approximately parallel to the undisturbed bands but shifted relative to the undisturbed bands in a direction normal to the bands.

Profile I: $t/l = 0.658$ and 0.824, figures 4 to 13. - Profile I operates in the turbine with a spacing ratio $t/l = 0.676$. This spacing ratio lies between the values $t/l = 0.658$ and 0.824.

The flow around this profile was investigated at six different inlet-air angles with the smaller spacing ratio and at four different inlet-air angles with the larger spacing ratio.

Figure 4 shows the interference photograph made with $t/l = 0.658$ and the inlet-air angle $\beta_1 = 20^\circ$. In this case, the inlet-air angle is substantially smaller than the exit angle. The flow is therefore retarded by the cascade. The flow had to be markedly retarded upon entering the channel between the blades if it was to fill this space completely. Because the flow cannot overcome the pressure rise connected therewith, it separates from the back of the blade behind the stagnation point. The dead-water region occupies about three-fourths of the flow channel. It is only on the concave side of the blade that a small region of satisfactory flow can be found, although the flow in the interblade channel is again accelerated. The blade was unheated when this photograph was taken. The pronounced separation may be seen in figure 4 on the back of the left-hand and center blades. The right-hand blade, however, behaves differently. It is not similarly supplied with an unobjectionable flow because the leading edge of the profile is too near the rear wall f of the air channel ahead of the cascade (fig. 2(a)).

Profile I was also investigated with both spacing ratios at the following inlet-air angles: $\beta_1 = 25^\circ$, 34°, 40°, and 48°; and with the smaller spacing ratio at $\beta_1 = 90^\circ$ in addition. The resulting photographs comprise figures 5 to 13.

At the inlet-air angle of 25°, a separation immediately behind the leading edge again appears with both spacing ratios (figs. 5 and 10). This separation is connected with the fact that the angle $\beta_1 = 25°$ is still too small for satisfactory flow relations and, conversely, it is also caused by the sudden transition in the curvature of the back contour. Apparently, in both cases the dead-water region narrows in the direction of the flow as far as the point where the arc turns into the straight line; thereafter the dead-water region again broadens. The dead-water region increases with the spacing; therefore, the flow losses increase.

With the next inlet-air angle, 34°, (figs. 6 and 11) at which the blade operates with approximately zero pressure drop across the lattice, a separation on the back behind the stagnation point still occurs. In figure 11 it is just possible still to recognize this separation in a discontinuity in the course of the bands near the surface of the profile. In both spacings, the dead water could have been observed more distinctly if the interference bands had been arranged to run at right angles to their actual direction in figures 6 and 11. The dead-water region is smaller than when $\beta_1 = 25°$ but it attains a considerable extent at the straight final portion of the back surface. Probably the long trailing edge of the blade could be somewhat shortened without changing the flow around the blade.

The next inlet-air angle, $\beta_1 = 40°$ (figs. 7 and 12), is the first one at which the separation from the back of the blade behind the stagnation point is almost entirely eliminated. The dead-water region at the straight final portion of the back surface is also smaller. When the inlet-air angle is increased to 48° (figs. 8 and 13), the relations become still better; the interference photographs show a separation on the back of the blade only at the point of transition from the arc contour to the straight-line portion of the back. This separation may be observed with both spacings.

If the inlet-air angle were to be increased still further, a separation would occur on the front side downstream of the leading edge. This phenomenon is especially unmistakable at $\beta_1 = 90°$ in figure 9; on the front side downstream of the impact point the flow does not follow the contour of the profile but separates at the leading edge. In this experiment, the blade equipped with the heating coil was not heated. On the basis of the interference photographs taken, profile I does not operate altogether satisfactorily in the range of inlet-air angles $\beta_1 = 30°$ to 33°.

This statement applies to both spacing ratios; with the larger spacing ratio the losses are greater. Even with $\beta_1 = 34^\circ$, certain losses must still be expected. Not until β_1 amounts to about 40° or more does the flow become satisfactory over the greater part of the back contour.

The separation occurring close behind the stagnation point at smaller inlet-air angles seems to influence markedly the flow at the point of transition from the curved contour to the straight portion. In any case, the sharpness of the profile nose is not recommended.

Profile II: $t/l = 0.638$ and 0.800. - Profile II was also investigated for two spacing ratios. The value specified, $t/l = 0.676$, lies between these two spacings. The investigation of this profile included the four inlet-air angles $\beta_1 = 25^\circ$, 34°, 40°, and 48°. The photographs obtained comprise figures 14 to 25.

On the basis of previous experience, a marked separation on the back of the blade near the impact point was to be assumed at $\beta_1 = 20^\circ$. This separation is still present at $\beta_1 = 25^\circ$ although the dead-water region does become smaller. This is seen in figures 14, 18, and 19. Particularly at the larger spacing ratio the dead-water region is of large extent. At the next inlet-air angle $\beta_1 = 34^\circ$, the extent of the dead-water region does decrease but a separation on the back near the stagnation point still occurs as may be ascertained from the bend in the interference bands near the profile surface in figures 15, 20, 23, and 24. Here again the interference photographs indicate that the losses increase with increased spacing.

At the inlet-air angle $\beta_1 = 40^\circ$, a marked improvement already exists as compared with $\beta_1 = 34^\circ$. At only the larger spacing ratio does a small degree of separation seem to occur behind the leading edge (figs. 21 and 25); at $t/l = 0.638$, this separation of the flow is not unequivocally recognizable (fig. 16). Of course, in both cases a separation occurs at the point of transition from the arc contour to the straight final portion of the back surface; this separation is caused by the sudden change in the curvature.

At $\beta_1 = 48^\circ$ (figs. 17 and 22), the separation on the back near the stagnation point disappears in both spacing ratios and only the separation of flow at the straight final portion of the back surface remains. With further increase of the inlet-air angle, a separation on the front side of the profile would gradually develop; this development would again lead to greater flow losses.

From the comparison of the two profiles, it may be concluded that the flow around profile II is scarcely more favorable in spite of the rounding of the leading edge. Probably the radius of the rounding is too small to prevent a separation at inlet-air angles other than the most favorable one. The results obtained indicate a most favorable inlet-air angle that is in every case larger than the angle of shock-free entry derived in the usual manner from the profile drawing.

Translation by Edward S. Shafer,
National Advisory Committee
for Aeronautics.

REFERENCE

1. Eckert, E., and von Vietinghoff-Scheel, K.: Versuche über die Strömung durch Turbinenschaufelgitter. Vorabdrücke from: Jahrb. 1942 d. D. Luftfahrtforschung, Lfg. 5-6. Tech. Berichte, Bd. 9, Nr. 7, 1942.

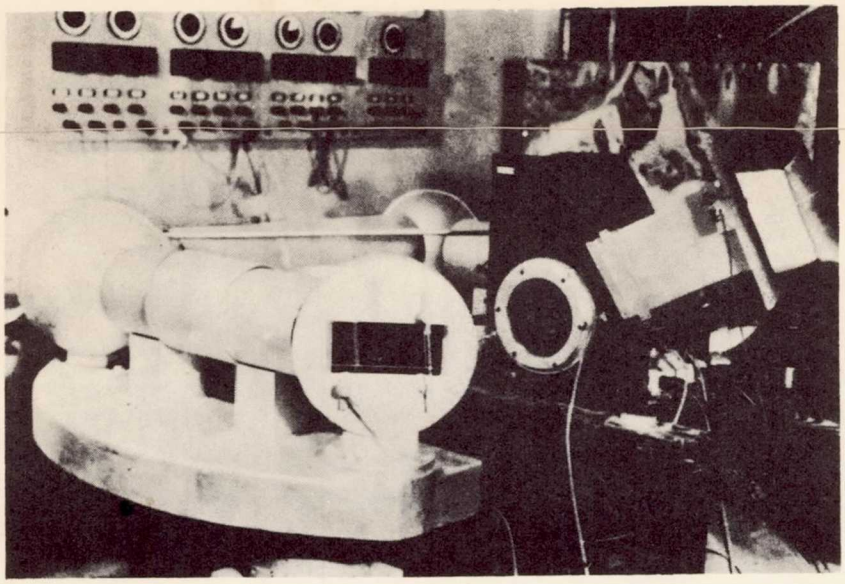

Figure 1

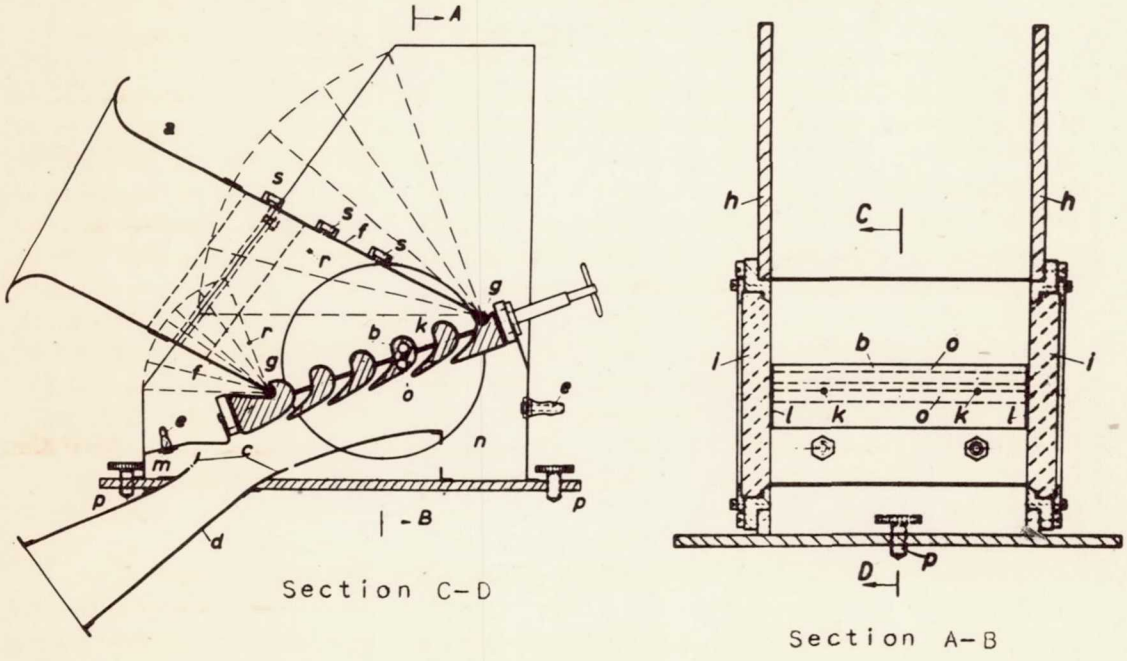

Figure 2

a Inlet duct
b Cascade
c Collecting funnel
d Diffuser
e Nipples for pressure-equalization lines
f Front and rear walls of inlet channel
g Axes upon which walls f turn
h Side walls
i Parallel-plane glass windows
k Tension wires
l Rubber pads
m,n Dead spaces
o Holes
p Adjusting screws
r Taps for pressure measurement
s Holes for pitot tube

Figure 3

Figure 4

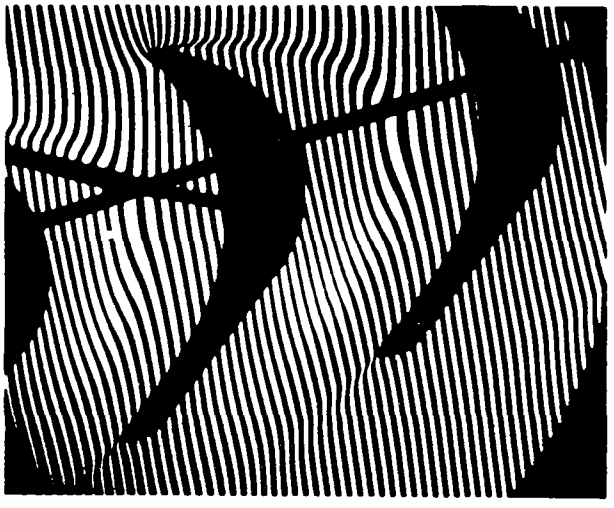

$t/s = 0.658$
$\beta_1 = 20^\circ$
$Re = 261,000$

Figure 5

$t/s = 0.658$
$\beta_1 = 25^\circ$
$Re = 294,000$

Figure 6

$t/\ell = 0.658$
$\beta_1 = 34^\circ$
Re = 283,000

Figure 7

$t/\ell = 0.658$
$\beta_1 = 40^\circ$
Re = 260,000

Figure 8

$t/\ell = 0.658$
$\beta_1 = 48^\circ$
Re = 230,000

Figure 9

$t/l = 0.658$
$\beta_1 = 90^\circ$
Re = 155,000

Figure 10

$t/l = 0.824$ [NACA comment: Value corrected from the German.]
$\beta_1 = 25^\circ$
Re = 279,000

Figure 11

$t/l = 0.824$
$\beta_1 = 34^\circ$
Re = 257,000

Figure 12

$t/l = 0.824$
$\beta_1 = 40^\circ$
Re = 241,000

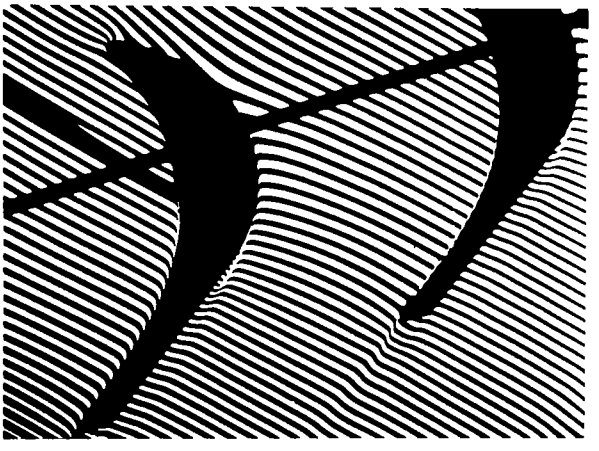

Figure 13

$t/l = 0.824$
$\beta_1 = 48^\circ$
Re = 216,000

Figure 14

$t/l = 0.638$
$\beta_1 = 25^\circ$
Re = 285,000

Figure 15

$t/\ell = 0.638$
$\beta_1 = 34^\circ$
Re = 271,500

Figure 16

$t/\ell = 0.638$
$\beta_1 = 40^\circ$
Re = 253,000

Figure 17

$t/\ell = 0.638$
$\beta_1 = 48^\circ$
Re = 215,000

Figure 18

$t/\ell = 0.800$
$\beta_1 = 25^\circ$
Re = 266,000

Figure 19

$t/\ell = 0.800$
$\beta_1 = 25^\circ$
Re = 266,000

Figure 20

$t/\ell = 0.800$
$\beta_1 = 34^\circ$
Re = 255,000

Figure 21

$t/\ell = 0.800$
$\beta_1 = 40^\circ$
Re = 246,000

Figure 22

$t/\ell = 0.800$
$\beta_1 = 48^\circ$
Re = 223,000

Figure 23

$t/\ell = 0.638$
$\beta_1 = 34^\circ$
Re = 271,500

Figure 24

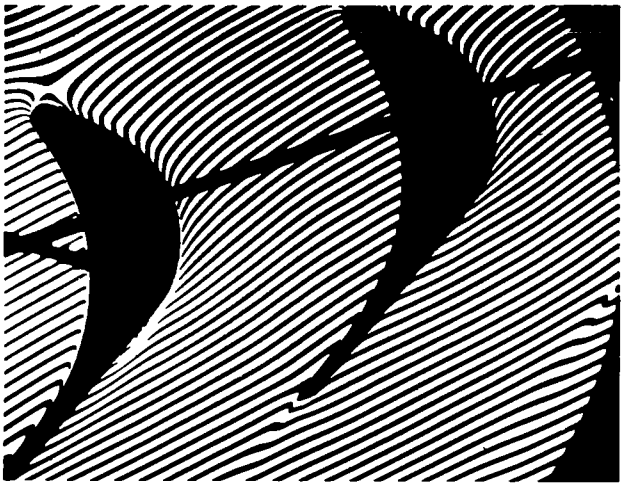

$t/\ell = 0.800$
$\beta_1 = 34^\circ$
Re = 255,000

Figure 25

$t/\ell = 0.800$
$\beta_1 = 40^\circ$
Re = 246,000